EUROPEAN FUSION DEVELOPMENT AGREEMENT

EFDA–JET–PR(03)09

Enzo Lazzaro and Paolo Zanca

Effects of a Non-Resonant m = 0 n = 1 Perturbation Driven by Coupling to the m = 2 n = 1 Mode in an Elongated Tokamak

Effects of a Non-Resonant m = 0 n = 1 Perturbation Driven by Coupling to the m = 2 n = 1 Mode in an Elongated Tokamak

Enzo Lazzaro and Paolo Zanca[1]

IFP-CNR, Associazione Euratom-ENEA-CNR per la Fusione, Via R. Cozzi 53, Milan, Italy
[1]Consorzio RFX, Associazione Euratom-ENEA-CNR per la Fusione, Corso Stati Uniti 4, Padova, Italy

Preprint of Paper to be submitted for publication in
Physics of Plasmas

ABSTRACT.

In a Tokamak the coupling of resonant tearing modes with the plasma shape effects like toroidicity, elongation and triangularity produces sidebands harmonics. In particular an m = 0, n = 1 non-resonant sideband can be driven by a m = 2, n = 1 tearing mode in an elliptic cross section Tokamak. It is shown that this is an important effect. The m = 0 mode is expected to produce a neoclassical toroidal viscous force which could explain the dramatic braking of the bulk plasma toroidal velocity observed during the onset of locked modes driven by resonant helical error fields or by spontaneous Magnetohydrodynamic (MHD) activity.

I. Introduction

The most developed configuration oriented to reach burning plasma regimes, the tokamak, is characterized in general by non-circular cross section that allows higher β limits. Furthermore the external power sources that provide the required auxiliary heating, can also inject a non-negligible momentum that drives a toroidal rotation of the bulk plasma. This effect is generally considered beneficial in limiting the onset of resistive magnetic reconnection phenomena that may evolve nonlinearly into helical magnetic islands that deteriorate energy confinement, or lead to disruptive collapse of the discharge. In fact the physics of plasma rotation, related to transport theory, and the physics of magnetic perturbations described by resistive MHD, have a common area that requires attention for the role it plays in guaranteeing reliability of tokamak performances. It has long been known from experiments that often naturally or externally driven helical magnetic field perturbations cause a dramatic quench of plasma toroidal rotation [1, 2] and consequent negative effects on confinement. These observations have so far not been totally satisfactorily explained and a purpose of this paper is to develop an adequate theoretical model that singles out the most relevant physical aspects of the problem, pointing out the role of coupling of modes associated to shaping effects. In a Tokamak with non-circular equilibrium magnetic surfaces, any MHD non-axisymmetric instability manifests several poloidal Fourier components, due to the coupling with the poloidal harmonics of the equilibrium quantities [3, 4]. An important instability in a tokamak is the $m=2, n=1$ tearing mode, where m and n are respectively the poloidal and toroidal Fourier number related to a flux co-ordinates system, which resonates at the $q=2$ surface. In an elongated tokamak the coupling between this mode and the $m=2$ equilibrium harmonic produces an $m=0, n=1$ non-resonant sideband. The $m=0, n=1$ mode appears as a long wavelength toroidal ripple, and in the context of the plasma rotation its effect can be relevant. In fact a promising candidate to explain the global plasma braking observed during the strong MHD activity is the neoclassical toroidal viscous force which establishes when the axisymmetry is broken by the magnetic perturbation. As pointed out in [1], the toroidal viscous force is mainly related to the *toroidal* field component of the perturbation. According to the standard tokamak ordering, while for an $m\neq0$ $n\neq0$ mode this component is smaller than the radial and

poloidal ones, for an $m=0$, $n\neq 0$ mode it is just the dominant component. Moreover the toroidal field $m=0$, $n\neq 0$ perturbation has a constant trend in the central part of the plasma, which agrees with the fact that the observed velocity braking is *global*. This work aims to compute the $m=0$, $n=1$ sideband generated by an $m=2$, $n=1$ tearing mode by means of a relatively simple analytical approach, which is described in Sections II, III. In Section II the equilibrium model and the appropriate flux co-ordinates are introduced. In Section III the helical field perturbations are considered and the equations which couples the driver $m=2$, $n=1$ tearing mode to its $m=0$, $n=1$ sideband; these equations are derived from the Ampere's law and the electromagnetic torque balance condition written in curvilinear co-ordinates. This approach can be seen as an appropriate simplification of the more general theory presented in Ref.4 An explicit computation with the derived equations is shown in Section IV.

In Section V the equation of toroidal rotation is presented, including as a novel item the neoclassical toroidal viscous force arising when axisymmetry is destroyed by helical perturbations. The structure and role of this force is discussed and it is compared with typical experimental observations. For definiteness, evidence from the Joint European Torus (JET) experiment is reported described in Ref.1. Concluding remarks are given in Section VI.

II. Equilibrium model

The problem addressed in the following paragraphs requires the use of curvilinear coordinates to account properly for toroidal and non circular shape effects, albeit with simplifications allowed by a careful ordering in a small parameter $\varepsilon \sim a/R \ll 1$. To this end it is convenient to present in detail the geometric representation of the equilibrium configuration in parametric form, and the construction of appropriate symmetry flux coordinates.

A. Flux co-ordinates and metric coefficients for a large aspect ratio Tokamak

Consider a large aspect ratio ($\varepsilon \equiv a/R_0 << 1$), low-$\beta$ ($\beta = o(\varepsilon^2)$) elongated Tokamak. If r is a flux surface label with a dimension of length, ϕ is the geometrical toroidal angle and θ is the geometrical poloidal angle about the magnetic axis ($r=0$), the co-ordinates $u^i \equiv (r, \theta, \phi)$ are related to the cylindrical co-ordinates (R, ϕ, Z) by the familiar parametric representation (see Ref.4)

1) $R = R_0 - r\cos\theta - \Delta(r) + E(r)\cos\theta + o(\varepsilon^2)$

2) $Z = r\sin\theta + E(r)\sin\theta + o(\varepsilon^2)$

Both the shift Δ and the elongation parameter E are assumed to be o(ε a) quantities. Triangularity is presently neglected for simplicity. The equilibrium quantities are retained up to o(ε). Note that the radial co-ordinate is referred to the axisymmetric magnetic surfaces, so $\nabla r \cdot \nabla\phi = 0$. Moreover $\nabla\theta \cdot \nabla\phi = 0$ by definition. The covariant metric tensor $g^u_{ij} = \frac{\partial \mathbf{x}}{\partial u^i} \frac{\partial \mathbf{x}}{\partial u^j}$ is:

3) $g^u_{rr} = 1 + 2\Delta'\cos\theta - 2E'\cos 2\theta + o(\varepsilon^2)$; ‘= d/dr;

4) $g^u_{\theta\theta} = r^2 + 2rE\cos 2\theta + o(\varepsilon^2)$

5) $g^u_{r\theta} = -r\Delta'\sin\theta + E\sin 2\theta + rE'\sin 2\theta + o(\varepsilon^2)$

6) $g^u_{\phi\phi} = R^2 = R_0^2\left(1 - 2\frac{r}{R_0}\cos\theta + o(\varepsilon^2)\right)$

The Jacobian is

$$7)\ \sqrt{g_u} = rR_0\left(1 - \frac{r}{R_0}\cos\theta + \Delta'\cos\theta - E'\cos 2\theta + \frac{E}{r}\cos 2\theta + o(\varepsilon^2)\right)$$

The contravariant representation of the equilibrium magnetic field is (see, for instance Ref.5)

$$8)\ \mathbf{B}_{eq} = F_0(r)\times\nabla\theta - \Psi_0(r)\times\nabla\phi + r\times\nabla\nu(r,\theta)$$

where ν is a function periodic and zero-average with respect to θ.

From the the co-ordinates (r, θ, ϕ) we pass to the flux co-ordinates $w^i \equiv (r, \vartheta, \phi)$ by defining a new poloidal-like angle [5]

$$9)\ \vartheta = \theta + \frac{\nu(r,\theta)}{F_0'} \equiv \theta + \lambda(r,\theta)$$

The contravariant representation of the equilibrium magnetic field becomes:

$$10)\ \mathbf{B}_{eq} = F_0(r)\times\nabla\vartheta - \Psi_0(r)\times\nabla\phi$$

$$11)\ B_{eq}^{\vartheta} = \frac{1}{\sqrt{g}}\frac{d\Psi_0}{dr};\quad B_{eq}^{\phi} = \frac{1}{\sqrt{g}}\frac{dF_0}{dr};\quad B_{eq}^{r} = 0;$$

$$12)\ q \equiv \frac{dF_0/dr}{d\Psi_0/dr} = \frac{B_{eq}^{\phi}}{B_{eq}^{\vartheta}} = O(1);$$

In these flux coordinates the field lines on a constant flux surface are straight lines with slope $d\vartheta/d\phi = 1/q$. The Jacobian in the flux co-ordinate system is related to the previous (7) by

$$13)\ \frac{1}{\sqrt{g}} \equiv r\times\nabla\vartheta\times\nabla\phi = \frac{1}{\sqrt{g_u}}\left(1 + \frac{\partial\lambda}{\partial\theta}\right)$$

Note that $\nabla\vartheta\cdot\nabla\phi = 0$. Therefore the contravariant and covariant metric tensors in the flux coordinates are

14) $$g^{ij} = \quad w^i \qquad w^j = \begin{pmatrix} g^{rr} & g^{r\vartheta} & 0 \\ g^{r\vartheta} & g^{\vartheta\vartheta} & 0 \\ 0 & 0 & g^{\phi\phi} \end{pmatrix};$$

15) $$g_{ij} = \frac{\partial \mathbf{x}}{\partial w^i} \; \frac{\partial \mathbf{x}}{\partial w^j} = g \begin{pmatrix} g^{\vartheta\vartheta} g^{\phi\phi} & -g^{r\vartheta} g^{\phi\phi} & 0 \\ -g^{r\vartheta} g^{\phi\phi} & g^{rr} g^{\phi\phi} & 0 \\ 0 & 0 & g^{rr} g^{\vartheta\vartheta} - \left(g^{r\vartheta}\right)^2 \end{pmatrix};$$

It should be noted that $g_{ik} \; g^{kj} = \delta_i^{\,j}, \quad g = \det[g_{ij}] = 1/\det[g^{ij}]$.

To obtain these tensor elements the function λ must be determined. We start from the observation that the equilibrium radial current is zero. From Ampere's law $\nabla \times \boldsymbol{B} = \mu_0 \boldsymbol{J}$ and (10) this condition becomes:

16) $$\mu_0 J^r_{eq} = \frac{1}{\sqrt{g}} \frac{\partial}{\partial \vartheta} \left[\frac{g_{\phi\phi}}{\sqrt{g}} \right] \frac{dF_0}{dr} = 0$$

Therefore

17) $$\frac{g_{\phi\phi}}{\sqrt{g}} = K(r);$$

From (6, 7, 13, 17) the following relations are obtained:

18) $$K(r) = \frac{R_0}{r} (1 + o(\varepsilon^2));$$

19) $$\frac{1}{\sqrt{g}} = \frac{1}{r R_0} \left(1 + 2 \frac{r}{R_0} \cos\theta + o(\varepsilon^2) \right);$$

20) $\lambda(r,\theta) = \Delta'\sin\theta - \frac{E'}{2}\sin 2\theta + \frac{E}{2r}\sin 2\theta + \frac{r}{R_0}\sin\theta + o(\varepsilon^2)$.

Note that λ is a *o(ε)* quantity, so the inverse of (9) can be written as $\theta = \vartheta - \lambda(r,\vartheta) + o(\varepsilon^2)$. Inserting this expression in (1, 2) the relation between the flux co-ordinates and the cylindrical co-ordinates is derived:

21) $R = R_0 - r\cos\vartheta - r\lambda(r,\vartheta)\sin\vartheta - \Delta(r) + E(r)\cos\vartheta + o(\varepsilon^2)$

22) $Z = r\sin\vartheta - r\lambda(r,\vartheta)\cos\vartheta + E(r)\sin\vartheta + o(\varepsilon^2)$

From (20, 21, 22) the metric tensor elements g_{ij} in the flux co-ordinates are easily derived

23) $g_{rr} = 1 + 2\Delta'\cos\vartheta - 2E'\cos 2\vartheta + o(\varepsilon^2)$

24) $g_{\vartheta\vartheta} = r^2 - 2\frac{r^3}{R_0}\cos\vartheta - 2r^2\Delta'\cos\vartheta + 2r^2E'\cos 2\vartheta + o(\varepsilon^2)$

25)

$$g_{r\vartheta} = -\frac{r^2}{R_0}\sin\vartheta - r\Delta'\sin\vartheta - r^2\Delta''\sin\vartheta + \frac{3}{2}E\sin 2\vartheta + \frac{1}{2}rE'\sin 2\vartheta + \frac{1}{2}r^2E''\sin 2\vartheta + o(\varepsilon^2)$$

26) $g_{\phi\phi} = R^2 = R_0^2\left(1 - 2\frac{r}{R_0}\cos\vartheta + o(\varepsilon^2)\right)$;

Finally the Jacobian (19) can be written

27) $\frac{1}{\sqrt{g}} = \frac{1}{rR_0}\left(1 + 2\frac{r}{R_0}\cos\vartheta + o(\varepsilon^2)\right)$;

Note that the *m=2* poloidal harmonic of the Jacobian (27) is a $o(\varepsilon^2)$ fraction of the symmetric part $1/\sqrt{g_0} \equiv 1/rR_0$. In the following *(m, n)* will indicate the Fourier harmonic with poloidal number *m* and toroidal number *n* for any quantity. Moreover the symmetric component, i.e. the *m=0, n=0* part, will be indicated by the suffix "0"

B. The force balance equation

The metric properties of the configuration chosen are not just a geometric prescription but an expression of the equilibrium conditions, expressed in the simplest case by the Equation $p = \mathbf{J} \times \mathbf{B}$, with the current ***J*** and the field ***B*** consistent with Ampere's law.

Given that the pressure is a flux function, the force balance equation for the equilibrium fields is

$$28)\quad \frac{dp}{dr} = \sqrt{g}\left(J^{\vartheta}_{eq} B^{\phi}_{eq} - J^{\phi}_{eq} B^{\vartheta}_{eq}\right)$$

where the equilibrium currents from Ampere's Law can be written as

$$29)\quad \mu_0 J^{\phi}_{eq} = \frac{1}{\sqrt{g}} \frac{\partial}{\partial r}\left[\frac{g_{\vartheta\vartheta}}{\sqrt{g}} \frac{d\Psi_0}{dr}\right] - \frac{1}{\sqrt{g}} \frac{\partial}{\partial \vartheta}\left[\frac{g_{r\vartheta}}{\sqrt{g}} \frac{d\Psi_0}{dr}\right];$$

$$30)\quad \mu_0 J^{\vartheta}_{eq} = -\frac{1}{\sqrt{g}} \frac{\partial}{\partial r}\left[\frac{g_{\phi\phi}}{\sqrt{g}} \frac{dF_0}{dr}\right]$$

Since we want to study the coupling between a *m=2, n=1* mode and the elongation, an equation for the elongation is needed. This can be derived from the *m=2* harmonic of (28), taking into account the Expressions(17, 24, 25, 27, 29, 30) and that $\beta = o(\varepsilon^2)$:

$$31)\quad E'' + \frac{E'}{r}\left[1 + 2r\frac{\Psi_0''}{\Psi_0'}\right] - 3\frac{E}{r^2} = o(\varepsilon^2)\ /a$$

Note that from (11, 27) the *m=2* harmonics of the equilibrium magnetic fields are fraction $o(\varepsilon^2)$ of the symmetric component:

$$32)\quad \left(B^{\vartheta}_{eq}\right)^{m=2} = \left(\frac{1}{\sqrt{g}}\right)^{m=2} \frac{d\Psi_0}{dr} = o(\varepsilon^2) B^{\vartheta}_0; \qquad \left(B^{\phi}_{eq}\right)^{m=2} = o(\varepsilon^2) B^{\phi}_0;$$

The same for the currents: from (17, 30) one gets

$$33)\quad \left(J^{\vartheta}_{eq}\right)^{m=2} = o(\varepsilon^2) J^{\vartheta}_0$$

and making use of the force balance Equation (28) it is possible to demonstrate that

$$34)\quad \left(J^{\phi}_{eq}\right)^{m=2} = q\left(J^{\vartheta}_{eq}\right)^{m=2} = o(\varepsilon^2) J^{\phi}_0$$

C. The renormalized fields

The actual calculations, both for the equilibrium and the perturbed quantities, are performed using the following renormalized fields

$$35)\quad \hat{B}^{\phi} = R_0 B^{\phi}; \quad \hat{B}^{\vartheta} = rB^{\vartheta}; \quad \hat{J}^{\phi} = R_0 J^{\phi}; \quad \hat{J}^{\vartheta} = rJ^{\vartheta}$$

which have the correct dimensions for magnetic field and current density respectively. The *m=0, n=0* components obeys the usual tokamak ordering:

$$36)\quad \hat{B}^{\vartheta}_0 = o(\varepsilon)\hat{B}^{\phi}_0;$$

$$37)\quad \mu_0 \hat{J}^{\vartheta}_0 = -\frac{d\hat{B}^{\phi}_0}{dr} = o(\varepsilon^2)\hat{B}^{\phi}_0 / a; \quad \mu_0 \hat{J}^{\phi}_0 = \frac{1}{r}\frac{\partial}{\partial r}\left(r\hat{B}^{\vartheta}_0\right) = o(\varepsilon)\hat{B}^{\phi}_0 / a;$$

Moreover it is convenient to divide the *m=0, n=0* current into a parallel component and a perpendicular pressure driven current:

38) $\mu_0 \hat{J}_0^{\vartheta} = \sigma(r)\hat{B}_0^{\vartheta} + h(r)\hat{B}_0^{\phi}; \quad \mu_0 \hat{J}_0^{\phi} = \sigma(r)\hat{B}_0^{\phi} - h(r)\hat{B}_0^{\vartheta};$

where the parallel and pressure driven contributions are

39) $\sigma(r) = \mu_0 \frac{\hat{\mathbf{J}}_0 \quad \hat{\mathbf{B}}_0}{\hat{B}_0^2} = o(\varepsilon)/a; \quad h(r) = \mu_0 \frac{dp/dr}{B_0^2} = o(\varepsilon^2)/a;$

III. Perturbations

A. General definitions

Adding a non-axisymmetric perturbation to the equilibrium (10), the contravariant representation of the magnetic field becomes:

40) $\mathbf{B} = F \times \vartheta - \Psi \times \phi$

41)

$$\Psi(r,\vartheta,\phi) = \Psi_0(r) + \sum_{\substack{n\neq 0 \\ m}} \psi^{m,n}(r) e^{i(m\vartheta - n\phi)}; \quad F(r,\vartheta,\phi) = F_0(r) + \sum_{\substack{n\neq 0 \\ m}} f^{m,n}(r) e^{i(m\vartheta - n\phi)};$$

Note that the fields Ψ, F can be identified with the covariant components of the vector potential: $A_{\phi} = -\Psi, \quad A_{\vartheta} = F$. The Fourier expansions (41) contains only n≠0 harmonics. The magnetic field components, which contain both the equilibrium and the perturbation, are:

42) $B^{\vartheta} = \frac{1}{\sqrt{g}} \frac{\partial \Psi}{\partial r}; \quad B^{\phi} = \frac{1}{\sqrt{g}} \frac{\partial F}{\partial r}; \quad b^r = -\frac{1}{\sqrt{g}} \left(\frac{\partial F}{\partial \phi} + \frac{\partial \Psi}{\partial \vartheta} \right)$

Inserting (40) in the Ampere's law, one obtain the corresponding current components:

43)

$$\mu_0 J^{\phi} = \frac{1}{\sqrt{g}}\frac{\partial}{\partial r}\left[\frac{g_{\vartheta\vartheta}}{\sqrt{g}}\frac{\partial \Psi}{\partial r} - \frac{g_{r\vartheta}}{\sqrt{g}}\frac{\partial \Psi}{\partial \vartheta} - \frac{g_{r\vartheta}}{\sqrt{g}}\frac{\partial F}{\partial \phi}\right] + \frac{1}{\sqrt{g}}\frac{\partial}{\partial \vartheta}\left[\frac{g_{rr}}{\sqrt{g}}\frac{\partial \Psi}{\partial \vartheta} - \frac{g_{r\vartheta}}{\sqrt{g}}\frac{\partial \Psi}{\partial r} + \frac{g_{rr}}{\sqrt{g}}\frac{\partial F}{\partial \phi}\right]$$

44) $$\mu_0 J^{\vartheta} = \frac{1}{\sqrt{g}}\frac{\partial}{\partial r}\left[\frac{g_{\phi\phi}}{\sqrt{g}}\frac{\partial F}{\partial r}\right] + \frac{1}{\sqrt{g}}\frac{\partial}{\partial \phi}\left[\frac{g_{rr}}{\sqrt{g}}\frac{\partial F}{\partial \phi} + \frac{g_{r\vartheta}}{\sqrt{g}}\frac{\partial \Psi}{\partial r} - \frac{g_{rr}}{\sqrt{g}}\frac{\partial \Psi}{\partial \vartheta}\right]$$

45) $$\mu_0 J^{r} = \frac{1}{\sqrt{g}}\frac{\partial}{\partial \vartheta}\left[\frac{g_{\phi\phi}}{\sqrt{g}}\frac{\partial F}{\partial r}\right] + \frac{1}{\sqrt{g}}\frac{\partial}{\partial \phi}\left[\frac{g_{r\vartheta}}{\sqrt{g}}\frac{\partial F}{\partial \phi} - \frac{g_{\vartheta\vartheta}}{\sqrt{g}}\frac{\partial \Psi}{\partial r} + \frac{g_{r\vartheta}}{\sqrt{g}}\frac{\partial \Psi}{\partial \vartheta}\right]$$

A quasi-equilibrium configuration can be described by the torque-balance Equation $\nabla \times (\mathbf{J} \times \mathbf{B}) = 0$, whose i-th component is written as

46) $$w^i \qquad (\nabla \times \mathbf{J} \times \mathbf{B}) = \mathbf{B} \quad J^i - \mathbf{J} \quad B^i = 0$$

It is evident that Expressions (42-45) couple the harmonics of Ψ, F to the $(k\neq 0,\ 0)$ harmonics of the metric tensor and the Jacobian. Moreover Equation (46) couples the non axisymmetric perturbations to the $(k\neq 0,\ 0)$ harmonics of the equilibrium fields $\mathbf{B}_{eq}$, $\mathbf{J}_{eq}$. This implies that an unstable $m,\ n\neq 0$ mode produces a series of secondary sideband harmonics $(m\pm k,\ n)$. The Fourier expansions (41) must therefore contain besides the intrinsically unstable modes all the sideband harmonics. The sidebands in turn couple with the equilibrium $(k,\ 0)$ harmonics and determine a modification to the unstable $m,\ n\neq 0$ mode. This second type of coupling is called back-coupling.

The most important instability in a tokamak is the $m=2,\ n=1$ resonant tearing mode. In an elongated tokamak this mode is therefore expected to produce an $m=0,\ n=1$ non-resonant sideband due to the coupling with the $(-2,\ 0)$ harmonics of the equilibrium quantities. The purpose of this work is to determine the radial profile of the $m=0,\ n=1$ sideband and to asses if it is a significant effect. To this aim it is not necessary to study the full-coupled

problem, which should include the back-coupling to the *m=2, n=1* mode, but the coupling terms can be retained only in the computation of the sideband harmonic. Likewise it is not important here to distinguish if the *m=2, n=1* is intrinsically unstable, due to the spontaneous MHD activity of the plasma (see Ref.2) or it has been driven by an external error field as in the recent experiment performed at JET [1, 6].

B. Unstable m≠0, n≠0 tearing mode

Consider an *m≠0, n≠0* resonant tearing mode. The back-coupling gives a higher order correction to this mode, so at the leading order of approximation we can neglect it. Therefore formulas (42-45) become

$$47)\quad b^{r\,m,n} = -\frac{im}{\sqrt{g_0}}\psi^{m,n} + \frac{in}{\sqrt{g_0}} f^{m,n};\quad b^{\vartheta\,m,n} = \frac{1}{\sqrt{g_0}}\frac{d\psi^{m,n}}{dr};\quad b^{\phi\,m,n} = \frac{1}{\sqrt{g_0}}\frac{df^{m,n}}{dr}$$

$$48)\quad \mu_0 j^{\phi\,m,n} = \frac{1}{\sqrt{g_0}}\frac{d}{dr}\left[\left(\frac{g_{\vartheta\vartheta}}{\sqrt{g}}\right)_0 \frac{d\psi^{m,n}}{dr}\right] - m^2\left(\frac{g_{rr}}{g}\right)_0\psi^{m,n} + mn\left(\frac{g_{rr}}{g}\right)_0 f^{m,n};$$

$$49)\quad \mu_0 j^{\vartheta\,m,n} = -\frac{1}{\sqrt{g_0}}\frac{d}{dr}\left[K(r)\frac{df^{m,n}}{dr}\right] - m\left(\frac{g_{rr}}{g}\right)_0\psi^{m,n} + n^2\left(\frac{g_{rr}}{g}\right)_0 f^{m,n};$$

$$50)\quad \mu_0 j^{r\,m,n} = \frac{i\,m}{\sqrt{g_0}}\left[K(r)\frac{df^{m,n}}{dr}\right] + i\,n\left(\frac{g_{\vartheta\vartheta}}{g}\right)_0\frac{d\psi^{m,n}}{dr};$$

and the *(m, n)* harmonic of the torque balance equation is

51)

$$\mathbf{B}_0\quad j^{i[m,n]} + \mathbf{b}^{[m,n]}\quad J_0^i - \mathbf{J}_0\quad b^{i[m,n]} - \mathbf{j}^{[m,n]}\quad B_0^i = 0;\quad x^{[m,n]} \equiv x^{m,n}(r)\ e^{i(m\vartheta - n\phi)}$$

The "*r*" component of (51) provides

52) $$\mu_0 j^{r\,m,n} = \mu_0 \frac{m J_0^{\vartheta} - n J_0^{\phi}}{m B_0^{\vartheta} - n B_0^{\phi}} b^{r\,m,n} \equiv \mu_0 L^{m,n} b^{r\,m,n}$$

From the definitions (35-39) one gets

53) $$\mu_0 L^{m,n} = \sigma + h \frac{m \hat{B}_0^{\phi} + n\varepsilon \hat{B}_0^{\vartheta}}{m \hat{B}_0^{\vartheta} - n\varepsilon \hat{B}_0^{\phi}} = o(\varepsilon)/a$$

Combining the first of (47), and (50, 52) the following relation is obtained

54) $$\frac{df^{m,n}}{dr} = -\frac{n}{m}\left(\frac{r}{R_0}\right)^2 \frac{d\psi^{m,n}}{dr} + \mu_0 L^{m,n} \frac{r}{R_0}\left(\frac{n}{m} f^{m,n} - \psi^{m,n}\right)$$

Taking into account (53), this relation implies $f^{m,n} = o(\varepsilon^2)\psi^{m,n}$, which corresponds to the standard tokamak ordering for an *m≠0, n≠0* mode. Therefore the radial field and the perturbed toroidal current can be simplified by neglecting the higher order terms involving $f^{m,n}$:

55) $$b^{r\,m,n} = -\frac{im}{\sqrt{g_0}}\psi^{m,n}; \qquad \mu_0 j^{\phi\,m,n} = \frac{1}{\sqrt{g_0}} \frac{d}{dr}\left[\left(\frac{g_{\vartheta\vartheta}}{\sqrt{g}}\right)_0 \frac{d\psi^{m,n}}{dr}\right] - m^2\left(\frac{g_{rr}}{g}\right)_0 \psi^{m,n};$$

Using (52, 55) the "φ" component of (51) can written as:

56) $$\frac{d}{dr}\left[\left(\frac{g_{\vartheta\vartheta}}{\sqrt{g}}\right)_0 \frac{d\psi^{m,n}}{dr}\right] - m^2\left(\frac{g_{rr}}{\sqrt{g}}\right)_0 \psi^{m,n} + \left(\mu_0 L^{m,n} \frac{dB_0^{\phi}}{dr} - \mu_0 \frac{dJ_0^{\phi}}{dr}\right) \frac{m\psi^{m,n}}{mB_0^{\vartheta} - nB_0^{\phi}} = 0$$

We have taken into account that the term involving $f^{m,n}$ gives a $o(\varepsilon^2)$ higher order contribution. By inserting the definitions (35-39) in (56), we recognize that some terms

prove to be $o(\varepsilon^2)\psi^{m,n}$. The leading order of approximation for (56) can therefore be simplified further as:

57) $$\frac{d}{dr}\left[r\frac{d\psi^{m,n}}{dr}\right]-\frac{m^2}{r}\psi^{m,n}-\frac{m\,r\hat{B}_0^{\phi}}{m\hat{B}_0^{\vartheta}-n\varepsilon\hat{B}_0^{\phi}}\frac{d\sigma}{dr}\psi^{m,n}=0$$

C. Sideband m=0, n=1

In the leading order of approximation only the coupling between the dominant unstable *m=2, n=1* mode and the elongation is taken into consideration. Moreover the coupling terms including $f^{2,1}$ are higher order and therefore discarded. In this case formulas (42, 44, 45) becomes

58)

$$b^{r\,0,1}=\frac{i}{\sqrt{g_0}}f^{0,1}-2i\left(\frac{1}{\sqrt{g}}\right)^{-2,0}\psi^{2,1};\quad b^{\vartheta\,0,1}=\frac{1}{\sqrt{g_0}}\frac{d\psi^{0,1}}{dr}+\left(\frac{1}{\sqrt{g}}\right)^{-2,0}\frac{d\psi^{2,1}}{dr};\quad b^{\phi\,0,1}=\frac{1}{\sqrt{g_0}}\frac{df^{0,1}}{dr}$$

59) $$\mu_0 j^{r\,0,1}=\frac{-i}{\sqrt{g_0}}\left[-\frac{g_{\vartheta\vartheta}^{0,0}}{\sqrt{g_0}}\frac{d\Psi^{0,1}}{dr}-\frac{g_{\vartheta\vartheta}^{-2,0}}{\sqrt{g_0}}\frac{d\Psi^{2,1}}{dr}+2i\frac{g_{r\vartheta}^{-2,0}}{\sqrt{g_0}}\Psi^{2,1}+\frac{o(\varepsilon^2)}{\sqrt{g_0}}\Psi^{2,1}\right]$$

60)

$$\mu_0 j^{\vartheta\,0,1}=\frac{-1}{\sqrt{g_0}}\frac{d}{dr}\left[K(r)\frac{df^{0,1}}{dr}\right]-\frac{i}{\sqrt{g_0}}\left[i\frac{g_{rr}^{0,0}}{\sqrt{g_0}}f^{0,1}+\frac{g_{r\vartheta}^{-2,0}}{\sqrt{g_0}}\frac{d\Psi^{2,1}}{dr}-2i\frac{g_{rr}^{-2,0}}{\sqrt{g_0}}\Psi^{2,1}+\frac{o(\varepsilon^2)}{\sqrt{g_0}}\Psi^{2,1}\right]$$

Remember that from (27) the *(-2,0)* harmonic of the Jacobian is of order $\left(1/\sqrt{g}\right)^{-2,0}=o(\varepsilon^2)\left(1/\sqrt{g_0}\right)$. In (59, 60) its contribution has been incorporated in the term $o(\varepsilon^2)\psi^{2,1}$. Instead from (23, 24, 25) the coupling terms $g_{ij}^{-2,0}\psi^{2,1}$ appears to be $o(\varepsilon)\psi^{2,1}$. Therefore in the leading order of (58-60) we can retain only these terms and discard the contribution related to $\left(1/\sqrt{g}\right)^{-2,0}$.

The *m=0, n=1* harmonic of the torque-balance Equation (46) is

61)

$$\mathbf{B}_0 \quad j^{i[0,1]} + \mathbf{b}^{[0,1]} \quad J_0^i - \mathbf{J}_0 \quad b^{i[0,1]} - \mathbf{j}^{[0,1]} \quad B_0^i + \mathbf{B}^{[-2,0]} \quad j^{i[2,1]} + \mathbf{b}^{[2,1]} \quad J^{i[-2,0]} +$$

$$-\mathbf{J}^{[-2,0]} \quad b^{i[2,1]} - \mathbf{j}^{[2,1]} \quad B^{i[-2,0]} = 0$$

We shall consider the "r" and "ϑ" component of this equation. On the basis of (32, 33, 34) we are allowed to discard the last four terms of (61), which involve the coupling with the *(-2,0)* harmonic of the equilibrium field, because they provide a contribution $o(\varepsilon^2)\psi^{2,1}$. In the leading order approximation the "r" component therefore gives

62) $$j^{r\,0,1} = \frac{J_0^\phi}{B_0^\phi} b^{r\,0,1};$$

which by virtue of the first of (58) and (59) gives

63) $$\frac{d\psi^{0,1}}{dr} = \frac{1}{g_{\vartheta\vartheta}^{0,0}} \left[\mu_0 \frac{J_0^\phi}{B_0^\phi} \sqrt{g_0}\, f^{0,1} - g_{\vartheta\vartheta}^{-2,0} \frac{d\psi^{2,1}}{dr} + 2ig_{r\vartheta}^{-2,0} \psi^{2,1} \right]$$

Making use of (62, 63) the "ϑ" component of (61) leads to the following equation for $f^{0,1}$:

64) $$\frac{d}{dr}\left[\frac{R_0}{r}\frac{d}{dr} f^{0,1}\right] - f^{0,1}\left[\frac{g_{rr}^{0,0}}{\sqrt{g_0}} + \mu_0 \frac{J_0^\phi \frac{dB_0^\vartheta}{dr} - B_0^\phi \frac{dJ_0^\vartheta}{dr}}{B_0^{\phi\,2}} - \frac{\sqrt{g_0}}{g_{\vartheta\vartheta}^{0,0}}\left(\mu_0 \frac{J_0^\phi}{B_0^\phi}\right)^2\right] =$$

$$= \frac{d\psi^{2,1}}{dr}\left[\mu_0 \frac{J_0^\phi}{B_0^\phi} \frac{g_{\vartheta\vartheta}^{-2,0}}{g_{\vartheta\vartheta}^{0,0}} - i\frac{g_{r\vartheta}^{-2,0}}{\sqrt{g_0}}\right] - \psi^{2,1}\left[2\frac{g_{rr}^{-2,0}}{\sqrt{g_0}} + 2i\frac{\mu_0 J_0^\phi}{B_0^\phi}\frac{g_{r\vartheta}^{-2,0}}{g_{\vartheta\vartheta}^{0,0}}\right];$$

The Equations (63-64) completely specify the *m=0, n=1* perturbation. The *(-2,0)* harmonics of the metric tensors can be easily expressed in terms of the elongation by the expressions (23, 24, 25): making also use of the definitions (35-39), Eq.(64) can therefore be written as

$$(65)\quad \frac{d}{dr}\left[\frac{R_0^2}{r}\frac{d}{dr}f^{0,1}\right]-f^{0,1}\left[\frac{1}{r}-\frac{R_0^2}{r}\frac{\hat{B}_0^{\vartheta}}{\hat{B}_0^{\phi}}\frac{d\sigma}{dr}-\frac{R_0^2}{r}\sigma^2-\frac{R_0^2}{r}\frac{dh}{dr}+\frac{R_0^2}{r^2}h\right]=$$

$$=\frac{1}{4r}\frac{d\psi^{2,1}}{dr}\left[3E+rE'+r^2E''+4rR_0\sigma E'\right]+\frac{\psi^{2,1}}{4r^2}\left[2\sigma R_0\left(3E+rE'+r^2E''\right)+8rE'\right];$$

It is possible to demonstrate that Equation (65) can be obtained also from the set of equations discussed in the appendix of Ref.4 by neglecting coupling terms of order $o(\varepsilon^2)\psi^{2,1}$, as done in our derivation.

IV. Example of computation

A. Equilibrium fields

For sake of simplicity let's consider a zero-pressure equilibrium: therefore in (38) we set *h=0*. We take the following parameters suitable for JET: $R_0=3m$, $q_0=1$, $q_a=3.5$. The plasma boundary is assumed to be at *r=a=1.1m* (remember that the flux-surface label *r* has the dimension of length). In Fig.1 and Fig.2 a possible choice for the normalized parallel current profile $\sigma(r)\cdot a$, and the corresponding *q(r)* profile are respectively shown. All the computation have been performed with the "*Mathematica 4.0*" software[18]. The *q=2* surface is found at *r/a=0.7021*. We assume a flattening of $\sigma(r)$, introduced by means of the equilibrium model described in Ref.7. The choice is adequate to the purpose of this work. In fact, our aim is not to describe the time evolution of the mode, which would require the inner tearing layer analysis, rather to compute the radial profile associated to a

high-amplitude mode, such as for example a locked mode. In the high-amplitude non-linear regime it is known that the magnetic island causes a local flattening of the current profile nearby the rational surface. The $\sigma(r)$ profile adopted emulates this modification produced by the non-linear island physics (see, for example,Ref.8) and consequently resolves the singularity of the linear force balance Equation (57), avoiding the occurrence of poles in the poloidal and toroidal field perturbations approaching the rational surface (see Ref.7). Away from this surface the mode amplitude profile is negligibly affected by the assumptions made on the equilibrium parallel current.

The $m=0$, $n=0$ components of the renormalized toroidal and poloidal fields, i.e. $\hat{B}_0^{\phi}(r)$, $\hat{B}_0^{\vartheta}(r)$, are obtained combining Equations (37, 38). They are shown in Fig.3, where an on-axis value of 2T is assumed for the toroidal field.

The elongation Equation (31) is solved in the form

$$66)\quad \frac{d^2E}{dr^2}+\frac{1}{r}\frac{dE}{dr}\left(1+2r\frac{d\hat{B}_0^{\vartheta}/dr}{\hat{B}_0^{\vartheta}}\right)-3\frac{E}{r^2}=0;$$

to give the elongation radial profile. The boundary condition is assumed to be $E(a)=0.29m$, which is in the range of JET operation (b/a ~1.7). The profile so obtained is displayed in Fig.4.

B. The m=2, n=1 mode

The amplitude and phase (the phase is taken constant) of the mode are defined by $\psi^{21} \equiv \tilde{\psi}^{21}(r)e^{i\varphi^{2,1}}$. Equation (57) is solved for the mode amplitude profile in the free-boundary case (Fig.5). Therefore in the vacuum region we take $\tilde{\psi}^{2,1}(r) \quad r^{-2}$. A radial field of 1mT is assumed at the plasma edge $r=a$. In the example here considered this value corresponds to a ratio $b^r(a)/\hat{B}^{\vartheta}(a) \quad 0.5\%$, which is typical for locked modes at JET [2]. The edge value for the flux function is therefore $\tilde{\psi}^{21}(a)=\left|b^{r2,1}(a)\right|a\ R_0/2=1.65\ 10^{-3}T\ m^2$.

The poloidal and toroidal field (renormalized) are computed from Eqs.(47, 53, 54):

67) $\hat{b}^{\phi\,2,1} = \frac{1}{r}\frac{df^{2,1}}{dr} \quad -\frac{1}{2}\frac{r}{R_0^{\,2}}\frac{d\psi^{\,2,1}}{dr} - \frac{\sigma}{R_0}\psi^{\,2,1}; \quad \hat{b}^{\vartheta\,2,1} = \frac{1}{R_0}\frac{d\psi^{\,2,1}}{dr}$

Their amplitude profiles, obtained inserting in Eq.(67) the function $\tilde{\psi}^{\,2,1}$, are displayed in Fig.6.

C. The m=0, n=1 mode

Mode amplitude and phase (phase costant with *r*) are defined by $f^{\,0,1} \equiv \tilde{f}^{0,1}(r)e^{i\varphi^{\,0,1}}$. In the zero-pressure case Equation (65) becomes

68) $\frac{d}{dr}\left[\frac{R_0^2}{r}\frac{d}{dr}\tilde{f}^{\,0,1}\right] - \tilde{f}^{\,0,1}\left[\frac{1}{r} - \frac{R_0^2}{r}\frac{\hat{B}_0^{\vartheta}}{\hat{B}_0^{\phi}}\frac{d\sigma}{dr} - \frac{R_0^2}{r}\sigma^2\right] =$

$$= i\left[\frac{1}{4r}\frac{d\tilde{\psi}^{\,2,1}}{dr}\left[3E + rE' + r^2E'' + 4rR_0\sigma E'\right] + \frac{\tilde{\psi}^{\,2,1}}{4r^{\,2}}\left[2\sigma R_0\left(3E + rE' + r^2E''\right) + 8rE'\right]\right]e^{i\left(\varphi^{\,2,1} - \varphi^{\,0,1}\right)}$$

The boundary conditions are $f^{\,0,1}(0) = f^{\,0,1}(\infty) = 0$. The coupling expression in the r.h.s contains known functions, apart from the phase difference $\varphi^{\,2,1} - \varphi^{\,0,1}$, which must be zero or π, being all the other quantities real. A solution which satisfies the boundary condition is found only for $\varphi^{\,2,1} - \varphi^{\,0,1} = \pi$. The amplitude is shown in Fig.7.

From Eq.(58) the (renormalized) toroidal field perturbation is

69) $\hat{b}^{\phi\,0,1} = \frac{1}{r}\frac{df^{\,0,1}}{dr}$

From Eqs.(24, 25, 58, 63) the (renormalized) poloidal field perturbation can be written as

70) $\hat{b}^{\vartheta\,0,1} \quad \frac{1}{R_0}\frac{\partial\psi^{\,01}}{\partial r} = \frac{1}{r^2R_0}\left[R_0\sigma\,\tilde{f}^{\,0,1} + r^2E'\frac{d\tilde{\psi}^{\,2,1}}{dr} + \frac{1}{2}\left(3E + rE' + r^2E''\right)\tilde{\psi}^{\,2,1}\right]e^{i\varphi^{\,01}}$

To obtain Expression(70) we have taken into account that the harmonic $\left(1/\sqrt{g}\right)^{-2,0}$ gives a higher order contribution and that $\varphi^{2,1} - \varphi^{0,1} = \pi$. The perturbation amplitudes are reported in Fig.8: we can conclude that the *m=0, n=1* perturbation is an important effect. Note that the poloidal field amplitude is greater than the toroidal field one, by vitue of the coupling terms present in (70). In fact without these terms it would have been $\hat{b}^{\vartheta\,0,1} = \frac{\sigma}{r} f^{0,1} = o(\varepsilon)\hat{b}^{\phi\,0,1}$.

Equations (68) and (70) contain the essential message of the present work, namely the drive of toroidal "rippling" perturbations by sideband-mode generation in non circular cross-section tokamaks. The importance of this effect for reactor relevant scenarios, at high temperature and pronounced shaping can be judged from the results of a long sequence of occasional observations and recent results of dedicated experiments.

V. Anomalous braking of toroidal rotation

A. Experimental evidences

It has long been known that an anomalous fast bulk braking of plasma toroidal rotation in tokamaks can occur associated with low *m* number MHD locked modes but so far no satisfactory theoretical explanation has been provided (see for example Ref.2).

In a recent experiment performed at JET in shots with NBI momentum injection [1] the influence of an *m=2, n=1* locked mode on the *toroidal* plasma rotation was investigated. The *poloidal* plasma rotation is damped by neoclassical effects (poloidal viscous force) and it is not taken into consideration. The locked mode was induced by an error field generated by the internal saddle coils.

In Fig.9 the main features of that experiment are shown: a slow linear ramp of *m=2, n=1* error field, applied at $t = t_0$, produces an electromagnetic torque which brakes the toroidal plasma rotation at the q=2 surface (r/a≈0.7 in that discharge), while the plasma bulk remains unaffected. This is agreement with the standard theory for which a net electromagnetic torque develops at the rational surface only [9]. The angular toroidal

velocities at the different radii are normalized to the unperturbed values just before the application of the error field ($t= t_0$). Once the q=2 angular velocity has been halved at $t=t_{pen}$, it undergoes an abrupt stop, and the initally linear *br(t)* signal is non-linearly amplified, which means that a locked *m=2, n=1* island is formed. This process is called mode penetration, and it is well described by the standard theory [1,9]. The quite unexpected phenomenon is the rapid self-similar quench of the velocity in the whole plasma bulk, which starts just after the mode penetration and takes about 0.5s. The braking is self-similar because, with a good approximation, the ratio $\Omega^{\phi}(r, t) /\Omega^{\phi}(r, t_0)$ proves to be a function of time only. When the error field is switched off at $t\approx 59.5s$ the plasma recover the initial velocity profile sustained by the NBI injection with an analogous self-similar acceleration.

Now it can be shown that the theory developed in the previous paragraphs can provide a clue to the interpretation of the experimental evidence, as it relates to a rather neglected effect of pressure anisotropy in neoclassical regimes in a tokamak with non axisymmetric perturbations.

In most tokamak plasmas the observed cross-field particles and heat fluxes are dominated not by neoclassical transport, that describes the diffusion processes caused by binary Coulomb collisions between charged particles in toroidal magnetic confinement geometry, but by turbulent effects that cause anomalous transport. However transport fluxes tangential to the magnetic surfaces, such as poloidal and toroidal flows and bootstrap current are substantially in agreement with neoclassical theory predictions.

In the case of non-axisymmetric configurations neoclassical effects absent in axisymmetry appear, such as “ripple” transport and toroidal viscous forces. The viscous force is given by the divergence of the viscous stress tensor. The dominant part of the viscous stress has a Chew-Goldberger-Low form in all collisionality regimes [10], and manifests a pressure anisotropy that to lowest order is caused by the effect of flow against B:

$$\vec{\vec{\Pi}}_i = \left(p_{//} - p\right)\left(\hat{\mathbf{b}}\hat{\mathbf{b}} - \tfrac{1}{3}\vec{\vec{\mathrm{I}}}\right) \qquad (71)$$

$$\left(p_{//} - p\right) \quad -\frac{mn\mu\left\langle B^2\right\rangle}{\left\langle\left(\hat{\mathbf{b}} \quad B\right)^2\right\rangle}\mathbf{V} \quad \ln B \qquad (72)$$

Here B is the magnitude of the magnetic field, and the bracket stands for the flux surface average. The toroidal and poloidal viscous forces $\left\langle\hat{\mathbf{e}}_{\phi} \quad \vec{\Pi}_i\right\rangle$, $\left\langle\hat{\mathbf{e}}_{\vartheta} \quad \vec{\Pi}_i\right\rangle$ can be regarded as transport fluxes conjugate to the toroidal and poloidal flows $\langle\mathbf{V} \quad \phi\rangle / F'$, $\langle\mathbf{V} \quad \vartheta\rangle / \Psi'$ [11, 12, 13, 14]. The toroidal viscous force $\left\langle\hat{\mathbf{e}}_{\phi} \quad \vec{\Pi}_i\right\rangle$ vanishes exactly in axisymmetry but appears when the axisymmetry is broken by the helical perturbation. As the poloidal viscous force damps the poloidal flow, so the toroidal viscous force can brake the toroidal rotation in a non-axisymmetric configuration. Before mode penetration ($t < t_{pen}$,) the amplitude of the *m=2, n=1* plasma perturbation is small [9], so the neoclassical toroidal viscous force is negligible and only the electromagnetic torque localized at the q=2 surface acts. But after the mode penetration, with the formation of a magnetic island there is a sizeable increase of the *m=2, n=1* plasma perturbation amplitude and the neoclassical effect can become important. However, as pointed out in Ref.1,the toroidal viscous force associated to the *m=2, n=1* mode should not be sufficient to explain the observed self-similar braking: its effect, which mainly depends on the toroidal field perturbation, vanishes towards the plasma centre where instead an important braking is observed. Nevertheless the toroidal viscous force is particularly relevant for an *m=0* perturbation because its effect is more uniform in the plasma bulk. The reason is a different radial dependence of the perturbed quantities for *m=0* and *m≠0* modes: in particular the *m=0* toroidal field perturbation has a constant trend in the plasma centre (see Fig.8). So it has just been shown that in an elongated tokamak a significant *m=0, n=1* sideband is generated by an *m=2, n=1* driver. This sideband inherits the time dependence of the dominant *m=2, n=1* mode, so it appears and grows together the *m=2, n=1* perturbation after the mode penetration ($t \geq t_{pen}$,). During this phase a neoclassical toroidal viscous force related to both the *m=2, n=1* mode and the *m=0, n=1* sideband is therefore expected to influence the toroidal plasma flow. As discussed in Ref.6 the temporal sequence of Fig.9 suggests that this is indeed the

phenomenon which account for the observed braking. This effect is now investigated, improving the analysis described in Refs.1 and 6. The objective is not to perform a self-consistent simulation of the whole process 1) mode-locking, 2) global braking. In fact the first part of the problem can be considered already well understood. Rather the approach is simplified by giving an *m=2, n=1* locked mode as starting condition, and studying the consequent global velocity braking. In this context it is not important to discriminate if the locked mode has been externally produced like in the JET experiment, or it originated spontaneously (unstable plasma mode have the tendency to lock to the vessel wall and to the natural error field). In fact the rapid global velocity braking is observed also in the spontaneous MHD activity of the plasma [2]. In the previous section the magnetic perturbations have been computed for the free boundary case, because the presence of an error field produced by the saddle coils would have increased the complexity of the calculation.

B. Velocity equation

We attempt to describe the evolution of the toroidal velocity profile with the inclusion of the toroidal viscous force in the flux-surface averaged motion equation along the toroidal direction [1]:

$$73)\quad \rho\frac{\partial\Omega^{\phi}}{\partial t}-\frac{1}{r}\frac{\partial}{\partial r}\left[\mu\, r\frac{\partial}{\partial r}\left(\Omega^{\phi}-\Omega_0^{\phi}\right)\right]+\left[\frac{\pi^{1/2}p_i}{R_0 v_{Ti}}\sum_{m,n}\frac{\left(\hat{B}_0^{\vartheta}\,\hat{b}^{\vartheta\,m,n}+\hat{B}_0^{\phi}\,\hat{b}^{\phi\,m,n}\right)^2}{\hat{B}_0^4}\frac{n^2 q}{|m-nq|}\right]\Omega^{\phi}=0$$

Here $\Omega^{\phi}(r,t)\equiv\langle \boldsymbol{V}\cdot\nabla\phi\rangle$ is the averaged toroidal angular velocity profile, ρ is the density ,taken constant, and μ is the anomalous perpendicular viscosity taken with a constant value corresponding to a viscous decay time scale of about 0.5 sec. The function $\Omega^{\phi}_{0}(r)$ is the velocity profile at the instant of mode locking formation: as discussed before, this profile is assumed as starting condition. The related anomalous viscous term in Expression (73) represents with a good degree of approximation the NBI momentum input. The third term is the neoclassical toroidal viscous force $\left\langle \hat{\mathbf{e}}_{\phi}\quad \ddot{\Pi}_i\right\rangle/R_0$ in the

plateau collisional regime [11, 12] (p_i and v_{Ti} are the ion pressure and thermal speed respectively). For the moment we discuss this regime, that was already taken into consideration in a previous analysis of the braking problem [1]. On the basis of the more refined magnetic computations developed in the previous sections, it is easily shown that this expression is not adequate, and that a less collisonal regime must be adopted in order to explain the experimental braking observed at JET. Moreover in the region of the q=2 surface the plasma is estimated to be in the ion banana regime, with $\tau_i > \frac{R\, q(r)}{\varepsilon^{3/2} v_{thi}}$.

In the toroidal viscous force expression the two contributions related to the *m=2, n=1* mode and to the sideband *m=0, n=1* are added. Equation (73) is solved in the region between the magnetic axis and the *q=2* surface (which in the present equilibrium description is located at r/a=0.7021), where the effect of the *m=2, n=1* locked island is taken into account by imposing the vanishing of the toroidal rotation at the *q=2* surface. Therefore the imposed boundary conditions are:

$$74)\quad \Omega^{\phi}(r_s^{2,1}) = 0; \qquad \frac{\partial \Omega^{\phi}}{\partial r}(0) = 0$$

By defining $\hat{r} = r/a, \quad \tau_{\mu} = \rho a^2/\mu$, Equation (73) can be written as

$$75)\quad \frac{\partial \Omega^{\phi}}{\partial t} - \frac{1}{\tau_{\mu}} \frac{1}{\hat{r}} \frac{\partial}{\partial \hat{r}} \left[\hat{r} \frac{\partial}{\partial \hat{r}} \left(\Omega^{\phi} - \Omega_0^{\phi} \right) \right] + K(\hat{r}, t) \left(\Omega^{\phi} - \Omega_0^{\phi} \right) = 0$$

where

$$76)\quad K(\hat{r}, t) = \frac{\pi^{1/2} v_{Ti}}{2R_0} \sum_{m,n} \frac{\left(\hat{B}_0^{\vartheta}\, \hat{b}^{\vartheta\, m,n} + \hat{B}_0^{\phi}\, \hat{b}^{\phi\, m,n} \right)^2}{\hat{B}_0^4} \frac{n^2 q}{|m - nq|} \equiv \frac{\pi^{1/2} v_{Ti}}{2R_0} \sum_{m,n} M^{m,n}$$

As explained in Ref.1, if *K(r, t)* were a constant, say *K(r, t)=1/*τ_K, Equation (75) should admit a separable solution:

77) $$\Omega^{\phi}(\hat{r},t) = w(t)\ J_0\left(\frac{j_{01}}{r_s^{2,1}}\hat{r}\right)$$

where j_{01} is the first zero of the Bessel function J_0. The velocity would undergo an exponential self-similar exponential braking:

78) $$\frac{w(t)}{w(0)} = \frac{\tau_\mu \left(\frac{r_s^{2,1}}{j_{01}}\right)^2}{\tau_K + \tau_\mu \left(\frac{r_s^{2,1}}{j_{01}}\right)^2} \exp\left[-t\left(\frac{j_{01}}{r_s^{2,1}}\right)^2 \frac{1}{\tau_\mu} + \frac{1}{\tau_K}\right] + \frac{\tau_K}{\tau_K + \tau_\mu \left(\frac{r_s^{2,1}}{j_{01}}\right)^2}$$

The final stationary value depends on the relative strength of the perpendicular and neoclassical viscous coefficients.

The radial profiles of the magnetic geometrical factors $M^{2,1}$ and $M^{0,1}$, which enters in (76), computed using the perturbations obtained in the previous section, are shown in Fig.10: the $M^{2,1}$ term is more important near the q=2 surface, while the $M^{0,1}$ term compensates for the decreasing of $M^{2,1}$ in the central region of the plasma.

Therefore, if the temperature does not vary too much in the region taken into consideration the solution of Eq.(75) is expected to be comparable with the self-similar behaviour described by Eqs. (77, 78).

All the magnetic perturbations, and consequently *K(r, t),* inherit the time dependence of the *m=2, n=1* mode. The rate of forced magnetic flux reconnection for a locked island at the *m=2, n=1* rational surface, due to an external perturbation (mapped onto the plasma boundary), is described by the Rutherford equation [1, 9, 11, 15]

(79) $$\frac{d\tilde{\psi}_s}{dt} \approx \left(\frac{r^2}{\tau_R}\left(\frac{q' r \hat{B}_0^{\vartheta}}{4q}\right)^{1/2}\right)_{r=r_s^{2,1}} \left[\Delta_0' \sqrt{\tilde{\psi}_s} + \frac{2m}{r_s^{21}\sqrt{\tilde{\psi}_s}} \Psi_{ext}(t)\right]$$

where $\tilde{\psi}_s = \tilde{\psi}^{2,1}(r_s^{2,1})$ is the amplitude of perturbed reconnected flux on that surface, associated with an island half-width $W = \left(\tilde{\psi}_s\right)^{1/2}\left(4q/q'\, r\, \hat{B}_0'^{\vartheta}\right)^{1/2}\Big|_{r=r_s^{2,1}}$, and Δ_0' is the "natural" tearing mode instability index. In a case of a spontaneous instability, that is $\Delta_0'>0$ and $\Psi_{ext}=0$, the mode amplitude grows like t^2 and saturates due to the fact that the tearing stability index is indeed a function of W: $\Delta_0'(W) \quad \Delta_0'(0)\left(1-\frac{W}{W_{sat}}\right)$.

For the JET experiment described above, since no natural m=2, n=1 modes are observed, it is justified to assume that the condition of tearing stability $\Delta_0'\le 0$ holds. With an external driver $\Psi_{ext}(t)\propto t$, the amplitude $\tilde{\psi}_s$ grows approximately like $t^{4/3}$ so the toroidal viscous force $K(r, t)$ grows like $t^{8/3}$. When the error field is switched off ($\Psi_{ext}=0$), the amplitude $\tilde{\psi}_s$ should decrease with a parabolic time behaviour because $\Delta_0'\le 0$, although the dependence of Δ_0' on W could modify this trend.

Even though the perturbation radial profiles computed in the previous section are referred to the free-boundary case, the purpose is to mimic the time behaviour of the error field JET experiment. Therefore the magnetic perturbation is given the time dependence reported in Fig.11: this is the solution of Equation (79) with a parameter $\Delta_0'<0$ compatible with observations, and $\Psi_{ext}(t)\propto t$. The amplitude is normalized to the value of the final maximum perturbation, which is assumed to be the example computed in the previous Section 4. The growth phase is approximately proportional to $t^{4/3}$, and a subsequent parabolic decrease. The comparison with the magnetic signal displayed in Fig.9 is not straightforward, because in that case the contribution of the external error field is dominant.

Equation (75) is then solved adopting $v_{Ti} = 1.225\cdot 10^{5.5}$ *m/s*, which corresponds to a temperature of *1.5 KeV* in the plasma bulk, and with $\tau_\mu=(j_{01})^2$ *s* which implies a characteristic velocity damping time related to the perpendicular anomalous viscosity about *0.5s* (see formula 78). The starting profile is taken to be $\Omega_0^{\phi}(\hat{r}) = J_0\left(\frac{j_{01}}{\hat{r}_s^{2,1}}\hat{r}\right)$.

The time traces of the computed velocities, taken at different radii (the same of Fig.9) and normalized to the initial values, are shown in Fig.12. A self-similar braking when the mode amplitude grows, and a self-similar acceleration when the mode amplitude decreases are apparent because the traces essentially superimpose. The presence of the *m=0* mode in *K(r,t)* indeed accounts for the self-similarity. Nevertheless the final braking amplitude is too low compared to the values shown in Fig.9.

Having verified that the discrepancy is not related to a wrong choice for the anomalous perpendicular viscosity μ. This can be easily understood looking at Equation (78): under the same *K(r, t)*, the only way to have a significant final braking is to increase τ_μ up to unphysical values; moreover this would also lower the exponential braking rate, while the experiment shows very short time scales. Therefore the discrepancy is due to an underestimate of the neoclassical toroidal viscous force amplitude: we conclude that the plateau regime expression for the toroidal viscous force, adopted in Eqs.(73, 76), does not apply to the typical JET conditions. It is in fact likely that at high ion temperature a weaker collisional regime, for example the so called *1/ν* regime [13], is entered. In this regime numerical computations predict an increase of both the toroidal and poloidal viscous force [14] (see formula (38, 39) and Fig.5 of Ref.14). From the discussion presented in Ref.14 an analytical formula for the toroidal viscous force in the *1/ν* regime can be easily derived:

$$(80)\quad \left\langle \hat{\mathbf{e}}_\phi \quad \vec{\vec{\Pi}}_i \right\rangle_{1/\nu} \quad \frac{8}{3\sqrt{2}\pi^3}\frac{p_i \tau_{ii}}{R_0^{\,2}} \int_0^\infty dK \frac{K^4 e^{-K}}{H\left(K^{1/2}\right)} \frac{G^{(1/\nu)}}{q^2} \quad \left(R_0\,\Omega^\phi\right)$$

where $H(x) = \left[\left(2x^2 - 1\right) erf(x) + x\, erf'(x)\right] / (2x^2)$, and $G^{(1/\nu)}$ is a geometrical factor related to the magnetic perturbation, therefore the analogue of the terms $M^{m,n}$ given in (76) for the plateau regime. Unfortunately this expression has been developed for a toroidal configuration with a very low rotational transform and therefore is valid only in the limit *q>>1*. In the case considered here with *q~2* the condition *q>>1* appears extreme but for *q=O(1)* analytical expressions in the *1/ν* regime are not *easily* applicable. Nevertheless a comparison between formulas (73, 80) indicates that besides the effective

contribution of the different magnetic geometrical coefficients $M^{m,n}$, $G^{(1/\nu)}$, the enhancement expected in the $1/\nu$ regime should be of the order:

$$(81)\quad \frac{\langle \hat{e}_\phi \quad \vec{\Pi}_i \rangle_{1/\nu}}{\langle \hat{e}_\phi \quad \vec{\Pi}_i \rangle_{Plateau}} \qquad A \equiv \frac{8}{3\sqrt{2}\pi^3}\frac{p_i \tau_{ii}}{{R_0}^2 q^2}\int_0^\infty dK \frac{K^4 e^{-K}}{H\left(K^{1/2}\right)}\left(\frac{\pi^{1/2} p_i}{R_0\, \nu_{Ti}}\right) \approx \tau_{ii}\ \frac{\nu_{Ti}}{R_0\, q^2}$$

For the JET parameters $T \approx 1.5KeV$, $n \approx 10^{19} m^{-3}$ which characterize the error-field experiment, one gets $\tau_{ii} \approx$ 5 ms [16], and therefore A is about $646/q^2$. To summarize it has been shown that:

1) the neoclassical viscous force expressed by plateau-regime formula (73) with the contribution of both the driver $m=2$, $n=1$ and the sideband $m=0$, $n=1$ has substantially the correct radial dependence to explain the self-similar character of the braking.

2) the rate of braking evaluated in plateau regime appears quantitatively rather weak in comparison with observations, suggesting that the enhancement due to a less collisional regime should be considered. With the factor A defined by (81) in front of the plateau formula (76) the solution of Equation (75), displayed in Fig.13, exhibits a braking rate comparable with the experimentally observed one.

Note that the acceleration is more gradual than the braking, while from the experimental data of Fig.9 the two phenomena occur on similar time scales. The discrepancy could be due to an incorrect modeling of the mode spontaneous damping after the error field has switched off.

Repeating the last computation with the exclusion of $M^{0,1}$ term, therefore considering the only effect related to the $m=2$, $n=1$ mode, the self-similarity is lost and the braking effect is definitely weaker: as shown in Fig.14: in this case the relative braking is an increasing function of the radius. The conclusion is that if the toroidal viscous force has the radial dependence given by the plateau formula, the inclusion of the $m=0$, $n=1$ contribution is essential to obtain the self-similarity.

We can test the $1/\nu$ formula (80) valid for q>>1 configurations in the momentum balance equation. The geometrical magnetic factor $G^{(1/\nu)}$ is defined in Refs.13 and 14 , and in our notation it is approximately given by :

(82) $$G^{(1/\nu)}(r,t) \quad \frac{64}{9}\pi\left(\frac{r}{R}\right)^2\left|A^{0,1}-A^{2,1}\right|^{3/2}F\left(-\frac{3}{4},\frac{3}{2};2;-\frac{4A^{2,1}A^{0,1}}{\left(A^{0,1}-A^{2,1}\right)^2}\right)+$$

$$+2.736\,\pi\,\frac{\left(A^{2,1}\,A^{0,1}\right)^2}{\left|A^{0,1}-A^{2,1}\right|^{1/2}}F\left(\frac{1}{4},\frac{3}{2};3;-\frac{4A^{2,1}\,A^{0,1}}{\left(A^{0,1}-A^{2,1}\right)^2}\right);$$

where F is the hypergeometric function, and the quantities $A^{m,n}$ are similar to $M^{m,n}$:

(83) $$A^{m,n}(r,t)\equiv\frac{\hat{B}_0^{\phi}\,\hat{b}^{\phi\,m,n}+\hat{B}_0^{\vartheta}\,\hat{b}^{\vartheta\,m,n}}{\hat{B}_0^2}$$

Note that in (82) the perturbation enters with a power 3/2 instead of the power 2 of the plateau formula: this is another important factor of enhancement. The solution of the Equation of motion (75) with the toroidal viscous force given by Eqs.(80, 82, 83) is displayed in Fig.15: with respect to Fig.13 an even better agreement with the experimental trend of Fig.9 is obtained.

In this case the viscous force profile is less uniform radially than in the plateau regime, essentially because of the presence of the factor $(r/R)^2$ in the first dominant term of Expressioin (82). Nevertheless a quasi self-similar trend is again recovered due to the huge enhancement of this effect in the Expressions (80, 82). It has also been verified that imposing artificially $A^{2,1}$=0 in these formulas, thereby considering the only effect of the *m=0, n=1* mode, the result of Fig.15 is not significantly altered. Instead imposing $A^{0,1}$=0 the self similar character is partially lost: in particular the plasma centre is subject to a smaller braking. It can be concluded that also the toroidal viscous force (80) is mostly affected by the *m=0, n=1* sideband.

In conclusion the results presented highlight that both the radial structure of the coupled magnetic perturbations and the collisional regime considered have a strong influence on the braking of toroidal rotation. Concerning the former aspect it has been shown that in

an elongated tokamak the *m=2, n=1* tearing mode drives an *m=0, n=1* sideband and this gives an important contribution to the toroidal viscous force. In particular, if one adopts the radial dependence of the plateau regime formula, it makes this effect nearly uniform within the plasma thereby producing a self-similar velocity braking; nevertheless also using the 1/ν formula for q>>1 configurations the *m=0, n=1* sideband proves to produce the most significant effect. Concerning the collisionality there are indications for a strong enhancement of the toroidal viscous force passing from the plateau to the 1/ν regime, even if an analytical formula for the latter valid in *q=O(1)* configurations is needed to draw a more satisfactory comparison between the two regimes. In this context the high temperature long mean-free-path reactor regimes deserve attention since they are likely to enhance the effects of the non-axisymmetric viscosity related to a variety of causes, typically the unavoidable static toroidal ripple, in addition to the modes effects presented here.

As final remark we quote a recent analysis (see Ref.17) of the global velocity braking observed in DIII-D during the application of a multi-harmonic non-resonant n=3 error field. The proposed explanation, the ripple drag related to "transient time magnetic pumping", has a mathematical expression similar to the toroidal viscous force. Anyway a detailed comparison with the present analysis is not straightforward, mainly because the toroidal field perturbation amplitude computed here, which provides the dominant contribution to the toroidal viscous force, is significantly smaller than the effective perturbation amplitude responsible of the ripple drag as given in Ref.17.

VI. Conclusions

The successful operation of burning plasma experiments in tokamaks achieving stability against dissipative modes for a practical length of time encompassing many energy and momentum confinement times. The task demands a suitable control of magnetic field perturbations and plasma rotation. Here we have discussed the role of the unavoidable coupled mode structure of a non-circular toroidal magnetic configurations operating in reactor relevant low collisionality regimes. In particular we have presented here a mechanism of cross-interaction of magnetic perturbations and plasma flow that produce important observable effects, with strong impact on the confinement and stability issues.

Acknowledgements

This work was performed in the framework of the Italian Consiglio Nazionale delle Ricerche and the European Fusion Development Agreement.

References

[1] E. Lazzaro,R.J.Buttery,T,C.Hender, P.Zanca, R. Fitzpatrick,M. Bigi, T. Bolzonella, R. Coelho, M. DeBenedetti, S. Nowak, O. Sauter, M. Stamp,Physics of Plasmas, **9,**3906 (2002)

[2] J.A. Snipes, D. J. Campbell, P.S. Hughes *et al*, Nucl. Fusion **28,**1085 (1988);
J.A. Snipes, D.J. Campbell, T.C. Hender, *et al*, Nucl. Fusion **30**, 205 (1990)

[3] B.A.Carreras. *et al*, Nucl. Fusion **21,**511 (1981)

[4] R. Fitzpatrick, *et al*, Nucl. Fusion **33**, 1533 (1993)

[5] W.D D'haeseleer, W.N.G. Hitchon, W.I.van Rij, S.P. Hirshman and J.L. Shohet Flux Coordinates and Magnetic Field Structure (Springer-Verlag, NewYork, 1991)

[6] E. Lazzaro, P.Zanca, Proceedings of 29th European Physical Society Conference Montreux,2002,edited by R.Behn,C.Varandas,(European Physical Society,2002), Vol26B,p. xliv.

[7] P. Zanca, F. Sattin, Plasma Physics Controlled Fusion **45**, 1 (2003)

[8] L.S. Solov'ev, V.D. Shafranov, Review Plasma Physics **5** (1970), Chapter 1.

[9] R. Fitzpatrick, Nucl. Fusion, **33**, 1049 (1993)

[10] S. P. Hirshamn and D. J. Sigmar, Nucl. Fusion **21**, 1079 (1981).

[11] A.I.Smolyakov, A.Hirose, E.Lazzaro, G.Re and J. Callen,
Phys. Plasmas **2**, 1581 (1995)

[12] K.C.Shaing, S. P. Hirshman, and J. Callen Phys. Fluids **29**, 521 (1986)

[13] K.C.Shaing, S. A. Hokin, Phys. Fluids **26**, 2136 (1983)

[14] H. Sugama, S. Nishimura, Physics of Plasmas **9**, 4637(2002)

[15] X. Wang, A. Battacharjee, Phys. Plasmas **4**, 748 (1997)

[16] J. Wesson, Tokamaks, (Oxford Science Publications, Oxford, 1997)

[17] R. J. La Haye et al, Physics of Plasmas **9**, 2051 (2002)

[18] S. Wolfram, The Mathematica Book, (Cambridge University Press,Cambridge, 1996)

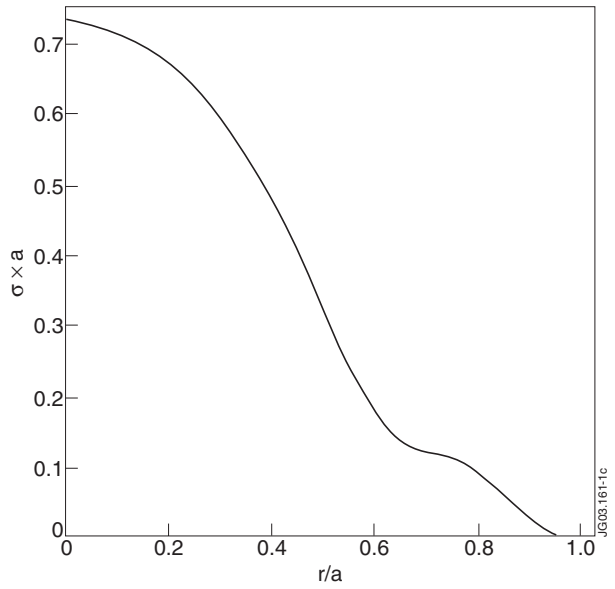

Fig.1: Normalized parallel current profile.

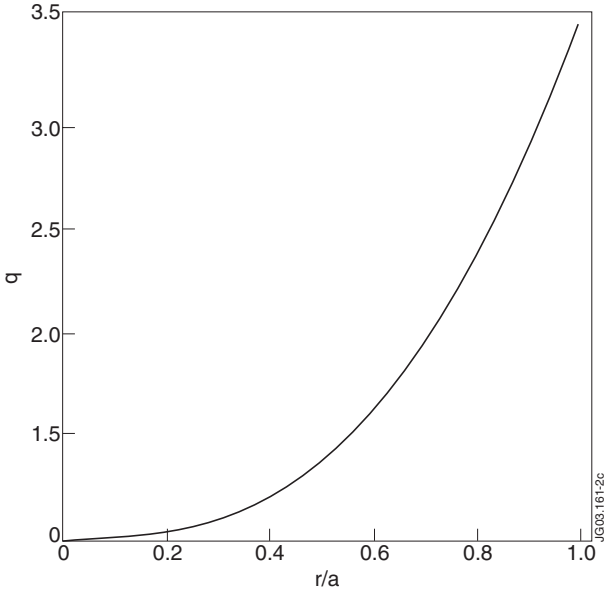

Fig.2: Safety factor profile.

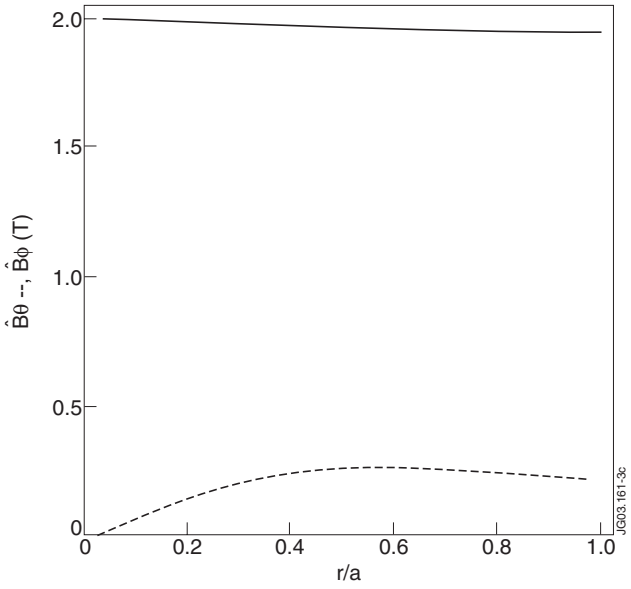

Fig.3: Toroidal (continuos line) and poloidal (dashed line) field profiles.

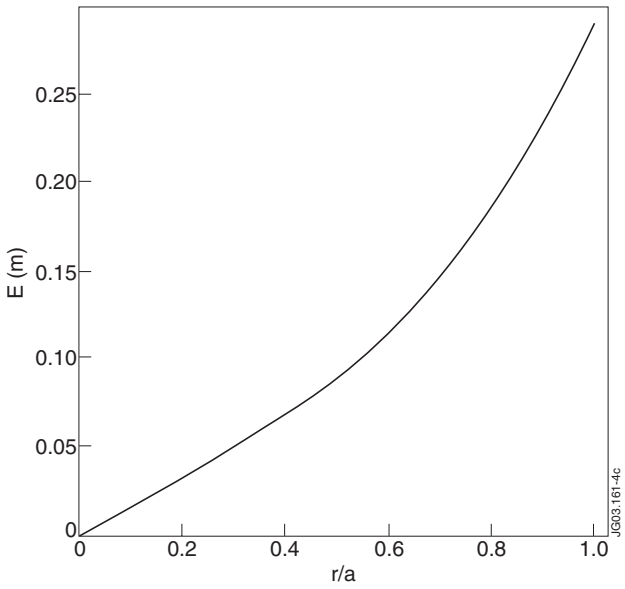

Fig.4: Elongation radial profile.

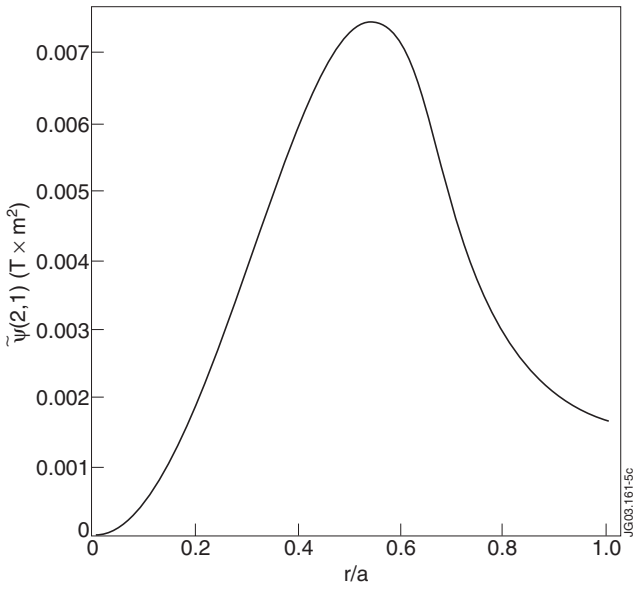

Fig.5: Radial profile of the m=2, n=1 mode amplitude.

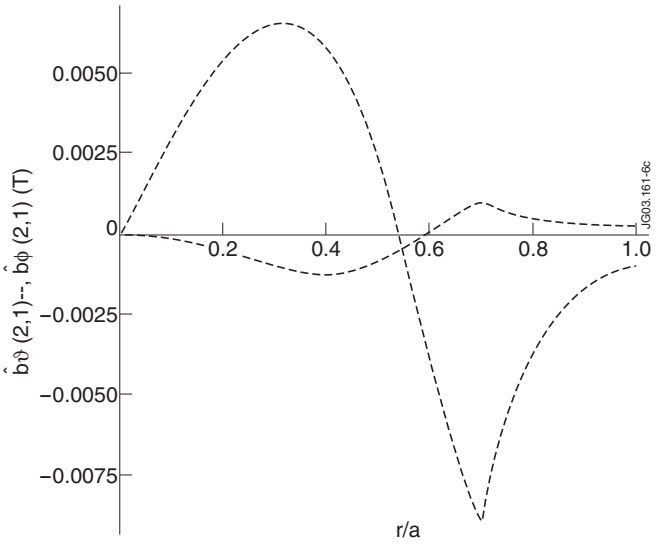

Fig. 6: Radial profiles of the m=2, n=1 toroidal (continuos line) and poloidal (dashed line) perturbations.

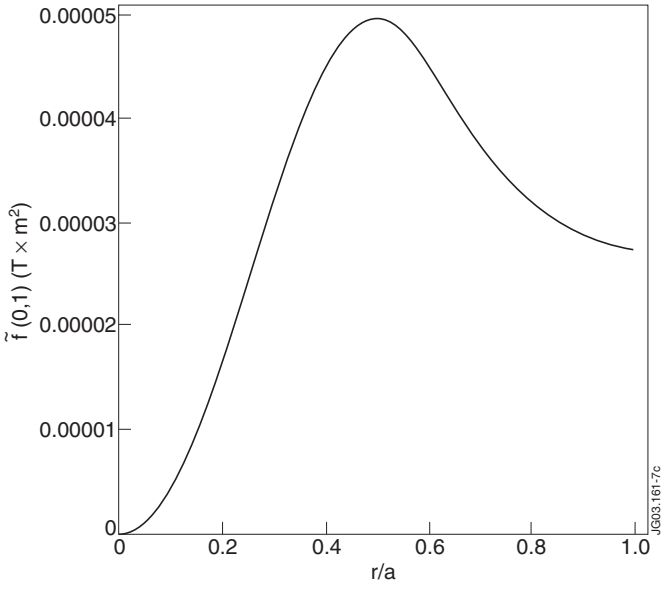

Fig.7: Radial profile for the m=0, n=1 mode amplitude.

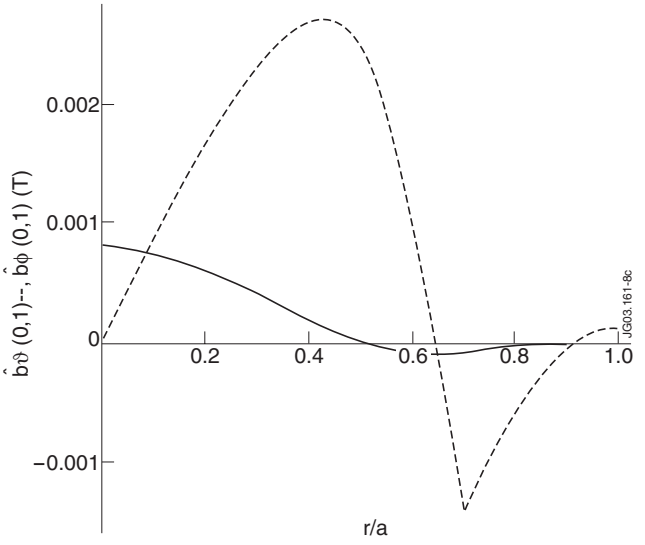

Fig.8: Radial profiles of the m=0, n=1 toroidal (continuos line) and poloidal (dashed line) perturbations.

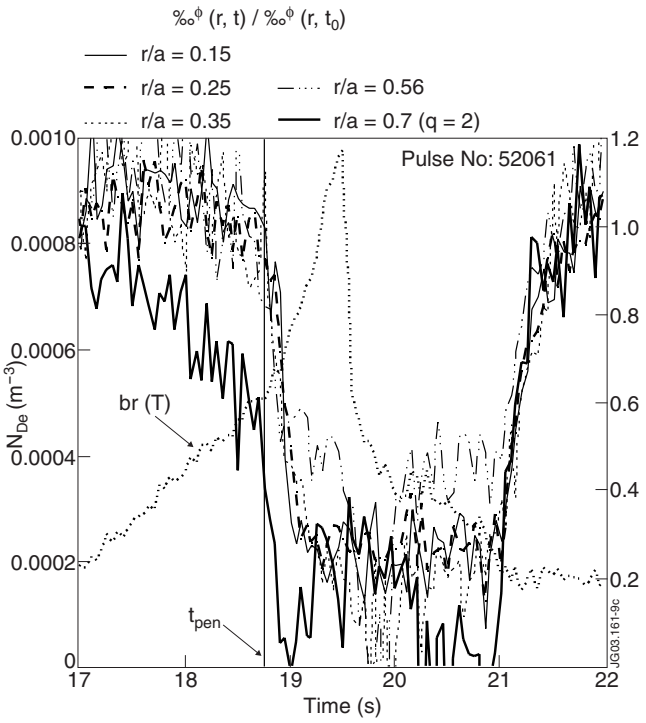

Fig.9: For a JET discharge: a) magnetic signal related to a m=2, n=1 error field; b) CXSM signals showing plasma toroidal rotation at different radii.

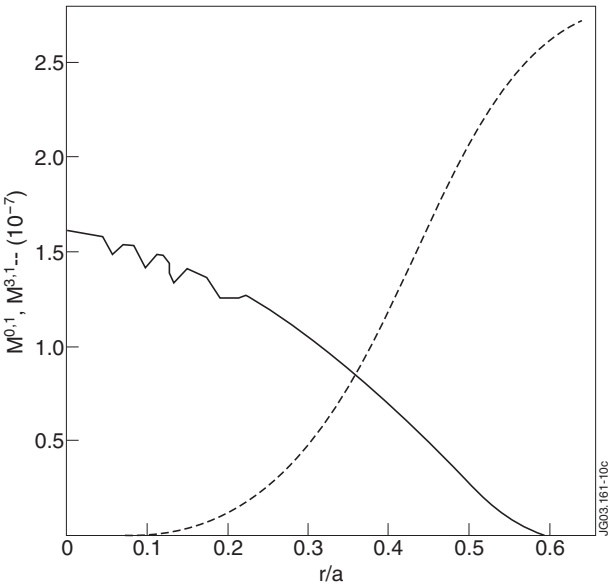

Fig.10: Radial profiles of the geometrical magnetic factors M m,n. Continuos line: M 0,1. Dashed line: M 2,1.

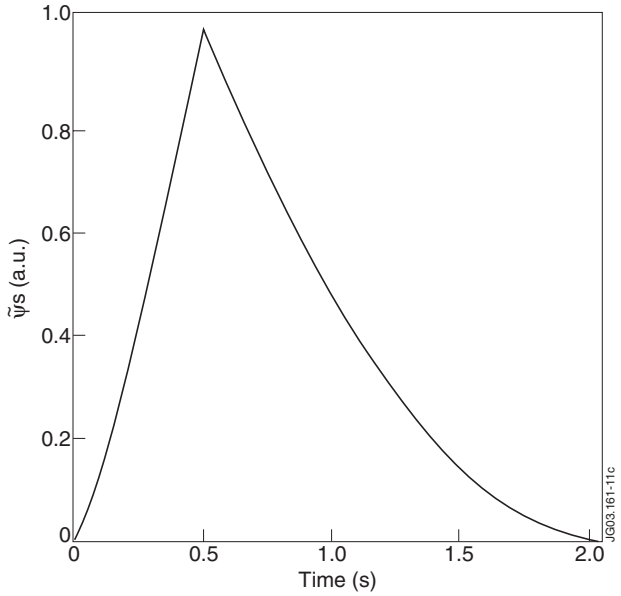

Fig.11: Ad-hoc time dependence given to the magnetic perturbation.

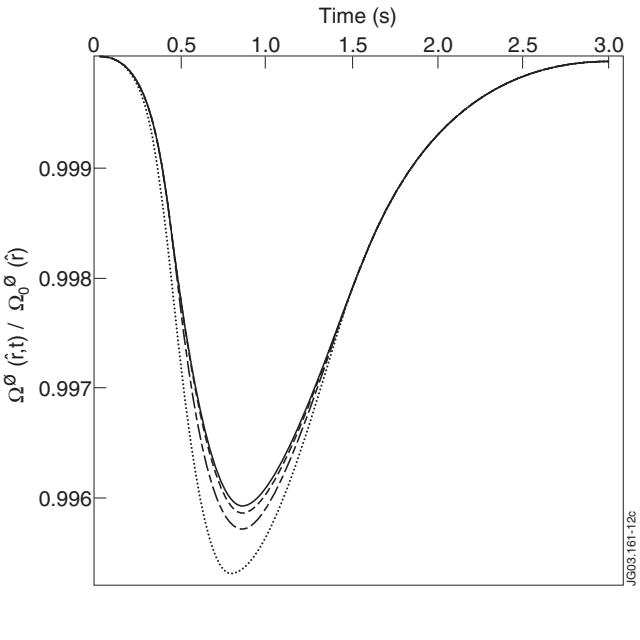

Fig.12: Normalized velocity time traces taken at different radii: r/a=0.15 (continuos line), r/a=0.25 (long dashed), r/a = 0.35 (medium dashed), r/a=0.56 (short dashed).

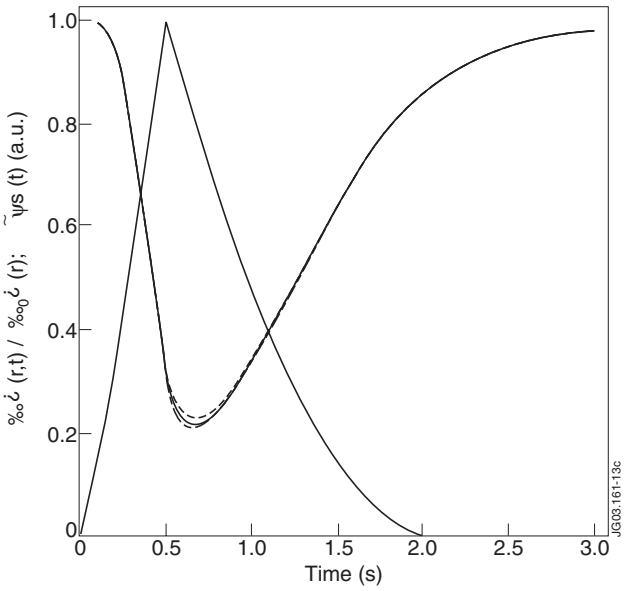

Fig.13: Dotted line: normalized mode amplitude. The other lines, which superimpose almost exactly, display the normalized velocity traces at the radii: r/a=(0.15, 0.25, 0.35, 0.56). The solution has been obtained with an enhancement factor A for the plateau regime toroidal viscous force. The braking rate and amplitude are comparable with the experimental ones.

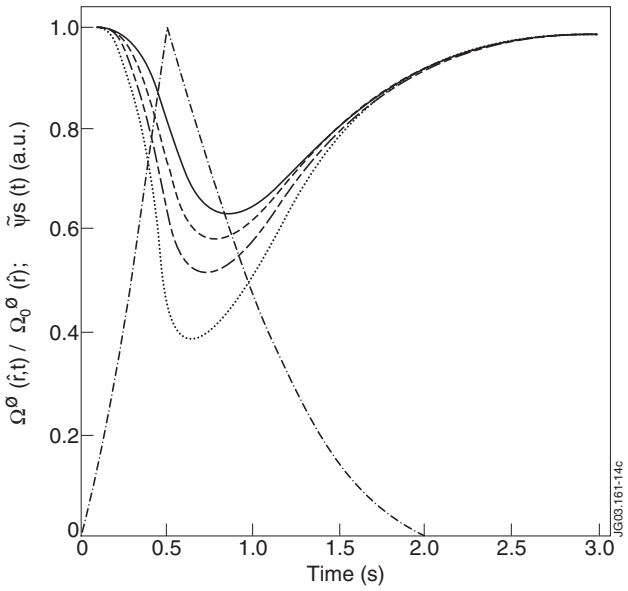

Fig.14: Same simbols of Fig.13. Dotted line: mode normalized amplitude. The other line display the normalized velocity traces at different radii: r/a=0.15 (continuous line), r/a=0.25 (long dashed), r/a = 0.35 (medium dashed), r/a=0.56 (short dashed). The solution has been obtained with an enhancement factor A for the plateau regime toroidal viscous force, but without the contribution of the m=0, n=1 mode.

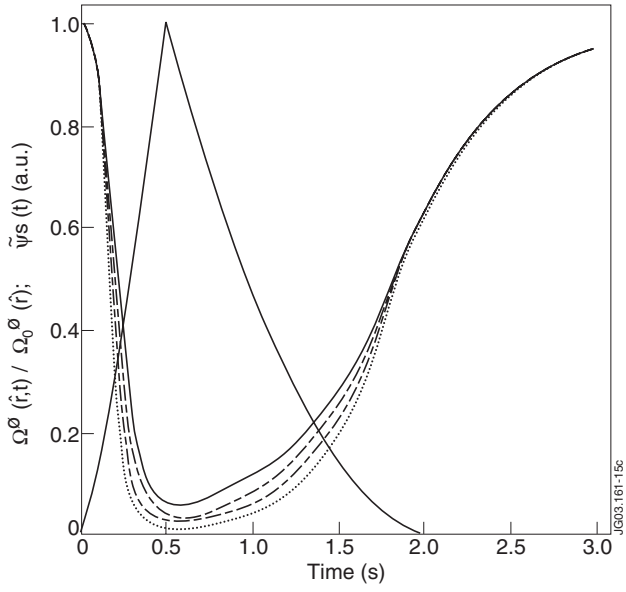

Fig.15: Same symbols Fig.14. In this case the toroidal viscous force defined by Eqs .(80-82) has been used.